A new educational approach to surface tension and Young-Laplace law by using computer-based simulations

A new educational approach to surface tension and Young-Laplace law by using computer-based simulations

Onofrio Rosario BATTAGLIA[0000-0002-0250-0514], **Giulia TERMINI**[0000-0001-8544-8274], **Aurelio AGLIOLO GALLITTO**[0000-0001-6617-9056] **and Claudio FAZIO**[0000-0002-3031-1665]
Dipartimento di Fisica e Chimica – Emilio Segrè, Università degli Studi di Palermo, Palermo Italy

onofriorosario.battaglia@unipa.it, giulia.termini01@unipa.it, aurelio.agliologallitto@unipa.it, claudio.fazio@unipa.it

Abstract. Here we present a pedagogical approach to surface tension phenomena based on a novel mesoscopic fluid model. We show that computer simulations based on this model can provide quantitative results that are consistent with experimental results. We simulate the formation of a two-dimensional liquid droplet without gravity and obtain its surface tension as a result by also verifying Young-Laplace's law. By controlling some simulation parameters, students can understand step by step how some physical quantities (e.g., the intensity of the interaction between two fluid particles) can affect the behaviour of fluids. This approach will provide students with an explicative model of surface phenomena.

1. Introduction

Traditional pedagogical approaches to surface phenomena often rely on a macroscopic description of the forces acting at interfaces and on a microscopic interpretation. Apart from sometimes being incorrect or contradictory, both approaches often prove ineffective in engaging students and fostering authentic understanding of physics content [1].

Our research aims to develop and test alternative strategies to improve the teaching and learning of surface phenomena, including the use of novel mesoscopic fluid models. In the scholarly literature, mesoscopic models are widely acknowledged for their efficacy in educational settings, particularly in facilitating the comprehension of fundamental concepts like surface tension. These models have the advantage over microscopic models in that they can explain surface tension using interparticle interactions, although they do not account for thermal fluctuations. In addition, mesoscopic models do not require many computational resources to successfully run the simulations. Therefore, teachers/students can even simulate large portions of fluids using computers commonly found in school laboratories.

We present here a mesoscopic fluid model and some computer simulation results based on this model. The simulations have been intentionally constructed to provide students with the ability to manipulate certain pertinent parameters within the model. We simulate the formation of a two-dimensional liquid droplet without gravity and determine its surface tension by also verifying Young-Laplace's law. This approach should allow students to become familiar with surface phenomena. By controlling some simulation parameters, students can understand step by step how some physical quantities (e.g., the

intensity of the interaction between two fluid particles) can affect the behaviour of fluids. This approach will provide students with an explicative model of surface phenomena.

2. The model

In this mesoscopic model, the fluid consists of particles whose size is much larger than that of a molecule (the radius of the particles is usually between 0.1 mm and 1 cm). The forces of interaction between mesoscopic particles exhibit analogous properties to those observed between microscopic particles. In very close proximity, they are repulsive, but at a distance, they are attractive. The intensity of this force is determined not only by the type of the two particles that are interacting with one another but also by the distance that separates them spatially. More specifically, the force's intensity is determined by whether the two particles that are interacting are liquid-liquid or solid-liquid. We solve the equations of our model by a numerical method called Smoothed Particle Hydrodynamics [3,4].

Smoothed particle hydrodynamics (SPH) is a computational technique that employs a Lagrangian approach to approximate solutions for the equations governing fluid dynamics. In this method, the fluid is represented by a collection of particles. The SPH method involves the assignment of physical properties, such as mass and density, to individual particles representing the fluid. The physical quantities are acquired through the process of interpolation.

The expression of a continuous quantity *Q(r)* as a function of position $\boldsymbol{r}$ can be mathematically represented by the following convolution integral.

$$Q(\boldsymbol{r}) = \int Q(\boldsymbol{r}')\delta(\boldsymbol{r} - \boldsymbol{r}')d\boldsymbol{r}' \tag{1}$$

where $\delta(\boldsymbol{r} - \boldsymbol{r}')$ is the Dirac Delta function.

In the SPH method, the Dirac Delta function is approximated using weighting functions, commonly referred to as *W*, in order to represent a generic smoothed quantity

$$Q_s(\boldsymbol{r}) = \int Q(\boldsymbol{r}')W(\boldsymbol{r} - \boldsymbol{r}', H)d\boldsymbol{r}'. \tag{2}$$

The weighting functions, denoted as *W*, play a crucial role in characterising the SPH method. These functions are defined within the range of *H*, which is also referred to as the "smoothing length". The variable $\boldsymbol{r}_i$ denotes the spatial location of the ith particle.

The interpolation integral in eq. (2) can be expressed as $Q_s(\boldsymbol{r}) = \int \frac{Q(\boldsymbol{r}')}{\rho(\boldsymbol{r}')} W(\boldsymbol{r} - \boldsymbol{r}', H)\rho(\boldsymbol{r}')d\boldsymbol{r}'$

where $\rho(\boldsymbol{r}')d\boldsymbol{r}'$ is a small portion of mass. Hence, in order to calculate the physical quantity associated to a generic particle *i*, the integral in eq. (2) is estimated through the subsequent summation [4].

$$Q_i = \sum_j m_j \frac{Q_j}{\rho_j} W(\boldsymbol{r_i} - \boldsymbol{r_j}, H) \tag{3}$$

where m_j, ΔV_j and ρ_j are the mass, the volume and the density of the particle *j*, respectively, and are functions of the position $\boldsymbol{r_j}$. The summation in equation (3) includes all particles in principle. However, the influence of the particle *i* is primarily limited to its immediate neighbouring particles, as the function *W* exhibits a rapid decrease in magnitude as the distance between particles increases.

The gradients of these quantities can also be approximated through a summation. The study of particle motion and its properties can be conducted through the utilisation of SPH formulations, which involve the replacement of quantities and their gradients in the Navier-Stokes equations. Numerous formulations of the

Navier-Stokes equations using SPH have been documented in the existing academic literature. [4]. The present study employs the following momentum-conservation equation, [5]

$$\frac{d\boldsymbol{v_i}}{dt} = -\sum_j m_j \left(\frac{P_j}{\rho^2{}_j} + \frac{P_i}{\rho^2{}_i}\right) \boldsymbol{\nabla_i}\, W(\boldsymbol{r_i} - \boldsymbol{r_j}, H) + \\ +2\eta \sum_j m_j \frac{(\boldsymbol{v_i} - \boldsymbol{v_j})}{\rho_i \rho_j (\boldsymbol{r_i} - \boldsymbol{r_j})^2} (\boldsymbol{r_i} - \boldsymbol{r_j}) \cdot \boldsymbol{\nabla_i}\, W(\boldsymbol{r_i} - \boldsymbol{r_j}, H) \tag{4}$$

where η is the dynamic viscosity, $\boldsymbol{v_i}$ and P_i indicate the velocity and the pressure of the generic particle *i,* respectively. The initial term on the right-hand side, which involves the SPH formulation of the pressure gradient, was derived by Lucy [3] and represents the acceleration resulting from the pressure force. The acceleration due to the SPH formulation of the viscous force, as derived by Morris et al. [6], is represented by the second term on the right-hand side. In the present model, the liquid exhibits weak compressibility, as this characteristic enhances the stability of the numerical evolution over time [7]. The pressure in equation (4) can be calculated by considering a state equation. The following Tait equation is employed for the determination of liquid pressure [8].

$$P = \frac{\rho c^2{}_0}{7}\left[\left(\frac{\rho}{\rho_0}\right)^7 - 1\right] \tag{5}$$

where c_0 is the sound speed, ρ is the density of the liquid and ρ_0 a reference density (in our analysis this value is fixed to 1000, in arbitrary units). The sound speed was established to be 50 times higher than the maximum velocity achievable by an SPH particle. This selection guarantees that variations in density can be regarded as insignificant [7]. The simulation incorporates the concept of "artificial viscosity" [7], a commonly employed technique in SPH algorithms to mitigate instabilities during the simulation process. The selection of the "artificial viscosity" parameter must be executed with great precision in order to achieve accurate estimations of the pressure within the droplet.

In order to accurately replicate surface tension phenomena, the model incorporated an additive force $\boldsymbol{F_{ij}}$ that considers the interactions between liquid particles and solid boundaries. Given the inherent relationship between surface tension and inter-molecular interactions, it is justifiable to incorporate an interaction force into the mesoscopic model that exhibits repulsion at close distances and attraction at greater distances. This force enabled the characterization of capillary phenomena and the examination of the interactions between liquid and solid particles that give rise to capillarity [9]. The magnitude of this force is contingent upon the separation between particles. In order to optimise computational efficiency and minimise the computational burden associated with inter-particle interactions, it is imperative to implement a cut-off on the range of these interactions. In the present investigation, the established threshold is defined as a distance equivalent to twice the value of *H*. The force referred to as the "molecular-like" force, as described by Tartakovsky and Meakin [5], is determined through the utilisation of a specific mathematical function reported below.

$$\boldsymbol{F_{ij}} = \begin{cases} S_{ij} cos\left(\frac{3\pi}{4H}|\boldsymbol{r_j} - \boldsymbol{r_i}|\right) & |\boldsymbol{r_j} - \boldsymbol{r_i}| \le 2H \\ 0 & |\boldsymbol{r_j} - \boldsymbol{r_i}| > 2H \end{cases} \tag{6}$$

S_{ij} and $|\boldsymbol{r_j}\text{-}\boldsymbol{r_i}|$ indicate the magnitude of the force between two particles *i* and *j* and the distance between them, respectively. This mathematical expression is similar to the one used by Tartakovsky and Meakin but with a support equal to 2*H* and not *H*. The force $\boldsymbol{F_{ij}}$ exhibits antisymmetry, denoted by $\boldsymbol{F_{ij}} = \text{-}\boldsymbol{F_{ji}}$, in accordance with the principle of momentum conservation. In the context of inter-particle interactions, it is observed that the force between particles is repulsive when the distance between them is less than 2⁄3 times

the characteristic length scale denoted as *H*. Conversely, when the inter-particle distance falls within the range of [2/3 *H*, 2*H*], the force becomes attractive. Finally, when the inter-particle distance surpasses 2*H*, the force between the particles becomes zero.

The significance of the short-range repulsive force in achieving liquid behaviour consistent with empirical observations has been duly acknowledged, as evidenced by numerous research findings [10,11,12].

In order to accurately calculate the total force exerted on a particle by all other liquid particles, the momentum equation is expressed as follows.

$$\frac{d\boldsymbol{v_i}}{dt} = -\sum_j m_j \left(\frac{P_j}{\rho^2{}_j} + \frac{P_i}{\rho^2{}_i}\right) \boldsymbol{\nabla_i} W(\boldsymbol{r_i} - \boldsymbol{r_j}, H) + 2\eta \sum_j m_j \frac{(\boldsymbol{v_i} - \boldsymbol{v_j})}{\rho_i \rho_j (\boldsymbol{r_i} - \boldsymbol{r_j})^2} (\boldsymbol{r_i} - \boldsymbol{r_j}) \cdot \cdot \boldsymbol{\nabla_i} W(\boldsymbol{r_i} - \boldsymbol{r_j}, H) + \frac{1}{m_i} \boldsymbol{F_i} \quad (7)$$

$\boldsymbol{F_i}$ is the whole force exerted on a particle *i* and calculated by using equation (6).

In this study, the researchers utilise a smoothing kernel function known as Wendland [7]. The polynomial function exhibits favourable characteristics in terms of resistance to tensile instability [13]. The calculation of time evolution is performed using a second-order method [7], which is a modified version of the leapfrog scheme [7].

3. Simulations Results

3.1. Droplet pressure vs radius

The pressure at mechanical equilibrium reached within a liquid droplet in the absence of gravitational forces is determined by the surface tension and the radius of the droplet, as described by the Young-Laplace law. At the onset of the simulation, the SPH particles are uniformly distributed in a rectangular configuration, with a separation distance of ds between adjacent particles. The experimental outcomes were acquired by establishing the following parameters: H = 0.48 mm, d_s = 0.16 mm as the initial interparticle distance, and S_{ij} = -1 × 10^{-5} a.u. as the liquid-liquid interaction force. Figure 1 illustrates the interparticle force, denoted as F_{ij}, based on the aforementioned parameters.

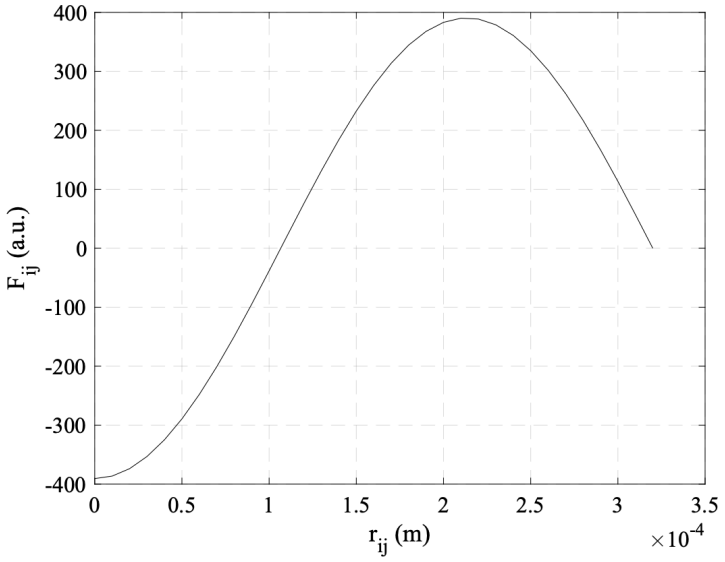

Figure 1. The dependence of the force per unit mass on interparticle distance r_{ij}.

A series of numerical experiments were conducted to investigate the formation of a two-dimensional liquid droplet in the absence of gravity. The experiments focused on observing the droplet formation as a function of its radius, and subsequently determining the corresponding surface tension values for each radius. Figure 2 illustrates an instance of a droplet in a state of static equilibrium, with emphasis placed on the molecular-like and pressure forces.

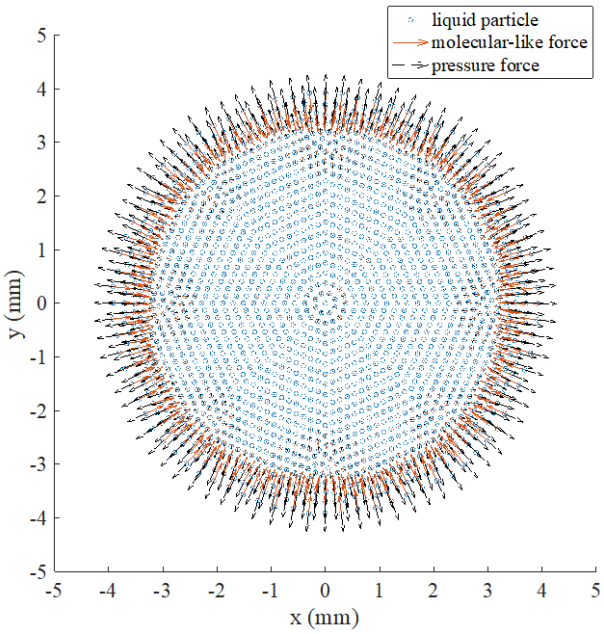

Figure 2. An illustration of a droplet in the state of mechanical equilibrium, derived from the outcomes of a simulation conducted across multiple time steps. Both the molecular-like and pressure forces are highlighted.

At the point of equilibrium, the simulation yields two key parameters: the pressure within the droplet and its corresponding radius.

The determination of surface tension involves the consideration of the widely recognised Young-Laplace equation in the context of two-dimensional systems, as reported below.

$$P_T = \frac{\sigma}{R} \tag{8}$$

σ is the surface tension, R the radius and P_T the pressure inside the drop.
At equilibrium, the pressure within the droplet is contingent upon the cumulative force exerted on each individual particle. According to Hoover (2014), it has been demonstrated SPH exhibits isomorphism with molecular dynamics, specifically in the context of particle-particle interactions involving multiple bodies. The utilisation of the SPH equations and the consideration of particle-particle interactions in a coherent manner enable the calculation of pressure based on the cumulative forces resulting from such interactions

$$P_T = P_k + \frac{1}{4\pi r^2}\sum_i \sum_j \mathbf{r}_{ij} \cdot \mathbf{f}_{ij}, \tag{9}$$

where P_k is the ideal gas (kinetic) contribution to the pressure, r is the "virial" radius of a circle inside the liquid drop and $\mathbf{f}_{ij}$ is the interaction force. In the scenario of a drop in a state of equilibrium, the value of P_k

is equal to zero. Similarly, the absence of viscous forces can be attributed to this condition. Therefore, the forces of interaction are

$$\mathbf{f}_{ij} = m_i m_j \left(\frac{P_j}{\rho_j^2} + \frac{P_i}{\rho_i^2} \right) \nabla_i W(\mathbf{r}_i - \mathbf{r}_j, H) + \mathbf{F}_{ij} \quad (10)$$

The summation includes all the particles located within the virial radius r (identified by the index i) and all the particles contained within the drop (identified by the index j). Exclusions are made for self-interactions.

Figure 3 illustrates the values of the pressure P_T, obtained through the utilisation of equation (9), in relation to the reciprocal of the radius R for various droplets of distinct sizes. Additionally, a linear regression analysis has been conducted employing the Young-Laplace law.

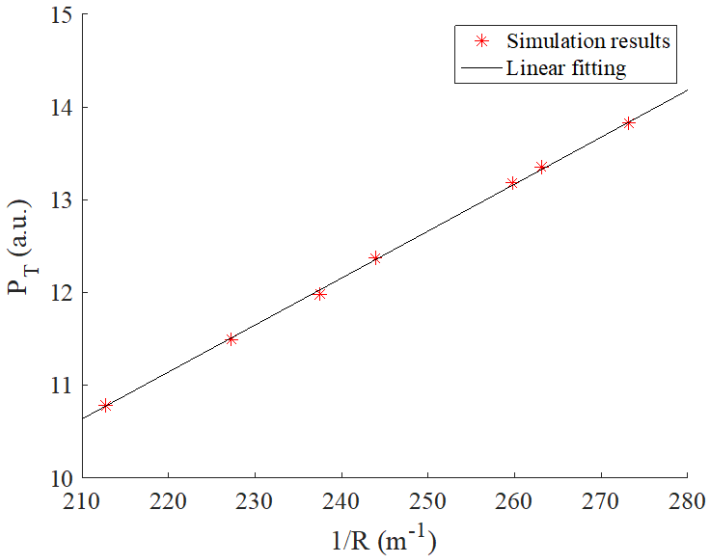

Figure 3. Droplet pressure values as a function of the inverse of the droplet radius and the linear regression.

Through the process of linear fitting, it is possible to make an estimation of the surface tension value (represented by the symbol σ) for the simulated liquid. The obtained value for the standard deviation, σ, is 0.05064 ± 0.00004 atomic units (a.u.). The coefficient of determination is approximately 0.99.

4. Discussion and Conclusions

The success of model-based approaches in physics learning has long been acknowledged in the literature (see, for example, [15]). Gilbert et al. recognised model creation in particular as a superordinate process skill [16] that can encourage the learner's critical thinking abilities. According to other research, including modelling activities in physics classes might help students develop a positive attitude towards learning the subject, make it easier for them to understand it, and help them recognise similarities and differences across a variety of occurrences [17,18,19].

According to research by Rutten et al., interactive simulations are an effective way to introduce modelling to students. It has been shown to be beneficial in generating learning that is meaningful for the learners to give students the opportunity to actively change model parameters and observe the results in real-time [20,21]. More specifically, the ability to solve problems and make decisions is crucial in simulation exercises. The pupils may have the chance to concentrate on the mechanism of functioning

behind the observable phenomena by step-by-step dissecting how the parameters connected to inter-particle interactions affect liquid behaviour. Students can learn how to use a model to anticipate results starting with tested hypotheses and gain an understanding of the value of the model building process through the use of simulations.

The simulation exercises that we developed are just one component of a larger teaching and learning sequence that also features significant hands-on, minds-on experimental activities as well as interactive courses that are based on active learning methodologies. Our sequence was tested with a defined group of high school students and the teachers who accompanied them; the findings of some of the pertinent components of that research are detailed elsewhere [22,23].

References

[1] Berry MV 1971 The molecular Mechanism of Surface Tension *Phys. Educ*. **6** 79-84.
[2] Besson U and Viennot L 2004 Using models at the mesoscopic scale in teaching physics: Two experimental interventions in solid friction and fluid statics *Int. J. Sci. Educ*. **26** 1083-1110.
[3] Lucy L B 1977 A numerical approach to the testing of the fission hypothesis *Astron J.* **82** 1013-24
[4] Monaghan J J 1992 *Annu. Rev. Astron. Astrophys* **30** 543-574
[5] Tartakovsky A and Meakin P 2005 Modeling of surface tension and contact angles with smoothed particle hydrodynamics *Phys. Rev.* E **72** 026301
[6] Morris J P, Fox P J, and Zhu Y 1997 Modeling Low Reynolds Number Incompressible Flows Using SPH *J. Comput. Phys.* **136** 214-226
[7] Monaghan J J 2005 *Rep. Prog. Phys.* **68** 1703-59
[8] Molteni D, Vitanza E and Battaglia OR 2017 Smoothed particles hydrodynamics numerical simulations of droplets walking on viscous vibrating liquid *Comput. Fluids* **156** *449-455*
[9] Battaglia OR, Agliolo Gallitto A, Termini G, Fazio C 2021 A study of capillarity phenomena by using a computer-based simulation approach *Eur. J. Phys.* **42** 055704
[10] Akinci N, Akinci G and Teschner M 2013 Versatile surface tension and adhesion for SPH fluids *ACM Trans. Graph.* **32** 182:1-182:8
[11] Tartakovsky AM and Panchenko A 2016 Pairwise Force Smoothed Particle Hydrodynamics model for multiphase flow: Surface tension and contact line dynamics *J. Comput. Phys.* **305** 1119-46
[12] Tartakovsky AM and Meakin P 2006 Pore-scale modeling of immiscible and miscible flows using smoothed particle hydrodynamics *Adv. Water. Resour.* **29** 1464–78
[13] Lang FM, Iglesias AS, Antuono M, and Colagrossi A 2011 *Proc. of 6th ERCOFTAC SPHERIC workshop on SPH applications* p. 30-37
[14] Hoover W G 1998 Isomorphism linking smooth particles and embedded atoms *Physica A* **260** 3-4
[15] Böttcher F, Meisert A 2011 Argumentation in Science Education: A Model-based Framework *Sci. & Educ.* **20** 103–140.
[16] Gilbert JK, Boulter C, Rutherford M 1998 Models in explanations: Part 1, Horses for courses? *Int. J. Sci. Educ.* **20** 83-97
[17] Zacharia ZC 2003 Beliefs, attitudes, and intentions of science teachers regarding the educational use of computer simulations and inquiry based experiments in physics *J. Res. Sci. Teach.* **40** 8 792–823
[18] Battaglia O R, Di Paola B, Fazio C 2017 K-means clustering to study how student reasoning lines can be modified by a learning activity based on Feynman's unifying approach *Eurasia J Math Sci T Educ* **13** 6 2005–2038
[19] Fazio C, Battaglia OR, Di Paola B 2013. Investigating the quality of mental models deployed by undergraduate engineering students in creating explanations: The case of thermally activated phenomena *Phys. Rev. ST PER* 2013 **9** 2 020101.

[20] Rutten N, Van Joolingen WR, Van der Veen JT 2012 The learning effects of computer simulations in science education *Comput. Educ.* **58** 136–153.
[21] Rutten N, Van der Veen JT, Van Joolingen WR 2015 Inquiry-based whole-class teaching with computer simulations in physics *Int. J. Sci. Educ.* **37** 8 1225–1245.
[22] Fazio C, Battaglia OR, Termini G 2022 Research-Based Design and Validation of a Teaching/Learning Sequence on Surface Phenomena *Proc. Int. Conf. 16th Frontiers of Fundamental Physics*: Fundamental Physics and Physics Education Online Conference. Istanbul 23-26 May 2022 (accepted for publication)
[23] Battaglia OR, Agliolo Gallitto A, Termini G, Fazio C 2023. Outcomes of a Teaching Learning Sequence on modelling surface phenomena in liquids *Ed. Sci.* **13** 425.